3D primary grain shapes resulting from semi-solid metal processing

U.A. Curle
Materials Science and Manufacturing, CSIR, Pretoria, South Africa. ucurle@csir.co.za

Abstract

The issue regarding globular grain shape and size has been a topic for semi-solid processing since the discovery of the technique. Semi-solid rheo-processing takes advantage of cooling a liquid metal alloy to the solid + liquid phase field, while it is subjected to some form of turbulence during cooling. It has been suggested that the grains grow into spherical globules by observations of 2D microstructures. It is also known that reducing the melt super-heat has the effect of reducing the globule (grain) size. Are these 2D globules also spherical in shape in 3D or are these 2D shapes remnants of the 3D shapes after sectioning along planes? An Al-Si-Mg alloy is semi-solid processed using a patented processing coil that induces contactless stirring while simultaneously being cooled. Primary aluminium grains are extracted by an etch technique from a sample volume of the casting. The grain size distribution and shapes are analysed. The 3D particles are pictured with scanning electron microscopy. Various interesting particle shapes are observed, from simple to complex. The particle geometry in 3D is compared to 2D optical light microscopy micrographs. It is found that the 2D globules are remnant shapes from the 3D particles after sectioning along random planes.

Keywords: Grain Morphology, Grain size, Roundness

1. Introduction

Commonly, semi-solid processing refers to processing of an alloy into the liquid + solid two phase region on a phase diagram before shaping. Thixo-processing indicates that an alloy was heated to this two phase region, while rheo-processing indicates that an alloy was cooled from above the liquidus temperature to this two phase region. Thixo-processing is mostly combined with a solid state forming process, e.g. forging, due to high solid fractions (~0.8) aimed for during thixo-processing. Rheo-processing is normally combined with a liquid shaping process, e.g. high pressure die casting (HPDC), due to the low solid fractions (~0.3) aimed for during processing. The semi-solid thixo-process has the disadvantage that it is a two-step process arising from initial alloy solidification resulting in a globular microstructure and then reheating. [1-6]

Most SSM process inventions are centred on rheo-processing in the light that it reduces cost over thixo-processing. Each new process invention has tried to show superiority by demonstrating the processing effect on globe size (mean grain size) and shape (roundness) [1-6].

The aim of this study was to investigate the grain size and shapes from a 3D perspective oppose to 2D micrograph analysis.

2. Experimental

A number of 1 kg castings of a bicycle suspension component were produced with the large scale CSIR R-HPDC cell (details of the process can be found in [7]). Alloy A356 was used with a composition (wt%) of 7.12 %Si, 0.35 %Mg, 0.09 %Fe, 0.14 %Ti and Al the balance. The alloy was not modified with Sr.

The solidification parameters for the process were: $T_{liquidus}$ = 613 °C, $T_{pouring}$ = 621 °C, manual transfer between furnace and rheo-processing coil, and 10 s rheo-processing time with a power of 4 kW.

The casting sequence was completed automatically once the metal processing finished. The cup was ejected from the coil and the robotic arm transferred the cup to the LK DCC630 shot control HPDC machine to complete the casting process. An oil heater controlling the die temperature was set to 160 °C.

One casting, in the as-cast condition, was selected to extract primary aluminium grains from. A square piece of ~10 g was sectioned out, from the runner part of the casting, and polished on all sides. A solution of 1:1 HCl to deionised H_2O was used to dissolve the eutectic component in between the primary aluminium grains. The sample was left in a plastic beaker overnight. The grains were three times washed with tap water and decanted each time. The grains were finally twice washed with ethanol and decanted. The beaker with the wet remaining grains was placed in a convection furnace at 50 °C to properly dry.

The 2D microstructure of the casting was imaged with a Leica DMI5000M inverted optical light microscope (OLM) equipped with a Leica DFC480 camera and Image-Pro MC v. 6.0 imaging software before the grains were

extracted. A Jeol JSM-6510 scanning electron microscope (SEM) was used to image the grains in 3D.

A particle size analysis were performed on OLM micrographs with ImageJ 1.50c software. Meanwhile a particle size analysis was also performed on the extracted aluminium grains using a Microtrac SIA image analysis system (SIA) combined with a Microtrac BLUEWAVE laser diffraction system. Data from the image analysis system was analysed with PartAn software.

3. Results and discussion

Figure 1 shows the 2D micrograph of the resultant microstructure after semi-solid metal processing. It can be seen that the grains have a rounded appearance, while there seem to be mixture of small and large grains. The grains also seem globular, meaning that the grains do not exhibit a dendritic appearance. The larger grains on the other hand have more rosettic features, being equi-axed.

Figure 2 shows some of the interesting shapes the primary aluminium particles have grown into throughout rheo-processing and casting. The 2D OLM micrograph is shown in Figure 2(a) as reference. The 3D grains corresponding to the 2D structures are identified by Figure 2(b) to Figure 2(i). The surface appearance of the 3D grains is generally rough, which is a consequence of the attack on the primary grain-eutectic interfaces by the extraction solution.

Figure 2(b) shows a grain that consists of two lobes and joined by a ligament. Figure 2(c) shows two different grains, one with two arms while the other has three arms. Channels are visible in between arms where the eutectic phase was located before extraction. Figure 2(d) shows a grain that has three protrusions. The protrusions don't have a clearly defined ligament but have thick "necks". Figure 2(e) is a good example of a compact equi-axed rosette. The dendrite arms have developed into "knobby" protrusions. Eutectic channels are again visible. Figure 2(f) shows that large elongated protrusions can also form, connected by thin ligaments. Figure 2(g) shows a grain that developed into a "fern-like" shape. Figure 2(h) shows a grain that developed into an open equi-axed rosette, again with a number of thick protrusions. Figure 2(i) shows that most simple shape of a sphere. A final comment, there seems to be only a few different basic shapes, each shape can range in size.

Particle size and shape analyses were performed using two different techniques, i.e. static image analysis with micrographs (OLM) and dynamic image analysis with a high speed camera (SIA). The dynamic image analysis should be more valuable than the static image analysis although the data obtained with both techniques is 2D in nature. The reason being that presentation to the detector of the particles has more random orientations due to the fact that the particles are dispersed in the liquid suspension medium. It could be well argued that the largest dimensions of the particles should be reported, unbiased by sectioning planes.

Table 1 shows the statistical results for the two image analysis techniques of the primary aluminium phase, OLM and SIA. The data set for the OLM is much smaller (~300 grains) than that for SIA (~6000 grains). The difference is so large because the number of grains that can be imaged at a specific magnification at a time is limited. The extracted grains are numerous. The laser diffraction results are not presented here because the diffraction caused by the defuse facetted particle surfaces under-estimates the particle size, resulting in even less meaningful information.

Table 1 also show that the statistics of the roundness and aspect ratio factors are similar with similar standard deviations. This observation could be attributed to the general relative roundness and shape of the grains in 3D. Roundish grains in 3D will appear roundish in 2D irrespective of the sectioning direction.

The mean aspect ratios with a value of ~1.5 for the grains given in Table 1 indicate that the grains are relatively elongated. The standard deviation of the OLM population is again larger which could be interpreted as the result of a view of a lower dimension of a higher dimension shape, depending on the plane of sectioning.

It can be seen that the mean of the ferret length in Table 1 is smaller for the OLM than for SIA, but is of the same order. The standard deviation of the population is also larger for OLM than for SIA. On face value it could be interpreted from the statistic results that there is only a marginal difference in the mean grain sizes measured by the two different techniques.

The question arises of how representative the summary statistics of the grain shapes and sizes are, and are the two techniques actually equivalent?

Figure 3 shows the ferret length for the two image analysis techniques in histogram form. It is clear that the results of OLM largely come from the smaller ferret size below 70 um. SIA has a relatively flat shape with almost even contributions between 60 um and 130 um. It has to be noted at this point that the size distributions deviate largely from a normal distribution precluding direct mean comparisons. This result is expected since 3D grains with protrusions and ligaments are cut along the sectioning planes which results in appearance of smaller 2D remnants of the grains.

From the above results it can be deduced that the 2D OLM technique under-estimates the actual grain size and that a larger range of grain shapes appear which is not the case in 3D.

The observations are related to solidification of the alloy during semi-solid processing in the following way. Copious heterogeneous nucleation takes place on the spout of the dosing furnace, especially with a low superheat above $T_{liquidus}$ in combination with turbulence in the pouring stream. Protrusions start to grow from nuclei during the static period (~3 s) while the metal in the cup is transferred to the rheo-processing coil. The nuclei with protrusions grow steadily into equi-axed grains during the vigorous stirring action of the magnetic field inside the coil with simultaneous forced air cooling. Growth of the primary grains in this alloy is unconstrained because of the

ratio of the liquid phase to the solid phase upon final solidification according to the phase diagram. Growth slows in the later part of processing due to the fact that most of the primary aluminium is consumed in the earlier stages of processing, with the result that further dendritic growth is suppressed during static periods. Solidification in the HPDC machine freezes the final microstructure.

Convection during solidification is very effective in limiting the directional growth of grains, in combination with low superheat pouring for copious nucleation. The grain shapes and sizes are very dependent on the specific process and accompanied processing parameters, e.g. $T_{liquidus}$, $T_{pouring}$, sites for heterogeneous nucleation, static time, processing time, stirring mechanism, stirring strength, and semi-solid fraction after processing.

On the side, some studies have indicated that small grains agglomerate during processing but the 3D grain shapes observed in this work would rather rationalise the 2D microstructures as finely branched equi-axed 3D grains than agglomerated grains.

4. Conclusions

Primary aluminium grains develop wonderful 3D shapes during the semi-solid process.

The results conclusively show that the true extracted 3D particle size and distribution is under-estimated by 2D image analysis using optical light microscopy, while also the particle shapes are over-estimated.

Copious nucleation and strong convection results in respectably equi-axed particles although protrusions are present (rosettes).

Acknowledgements

The author would like to thank the Department of Science and Technology (DST) for financial support under the Light Metals Development Network (LMDN) through the Advanced Metals Initiative (AMI). Continual support from the Advanced Casting Technology (ACT) research group leader, Dr Gonasagren Govender, is highly regarded.

References

1. Proc. 7th Internat. Conf on *Semi-Solid Processing of Alloys and Composites*, eds. Y. Tsutsui, M. Kiuchi, K. Ichikawa, 2002, pp.1-868.
2. Proc. 8th Internat. Conf. on *Semi-Solid Processing of Alloys and Composites*, Cyprus, 2004.
3. Proc. 9th Internat. Conf. on *Semi-Solid Processing of Alloys and Composites*, eds. C.G. Kang, S.K. Kim, S.Y. Lee, Korea, 2006. Solid State Phenomena 116-117 (2006) 1-797.
4. Proc. 10th Internat. Conf. on *Semi-Solid Processing of Alloys and Composites*, eds. G. Hirt, A. Rassili, A. Bührig-Polaczek, Germany, 2008. Solid State Phenomena 141-143 (2008) 1-978.
5. Proc. 11th Internat. Conf. on *Semi-Solid Processing of Alloys and Composites*, eds. W.D. Huang, Y.L. Kang, X.J. Yang, China, 2010. Transactions of Nonferrous Metals Society of China 20 (2010) 1556-1814.
6. Proc. 12th Internat. Conf. on *Semi-Solid Processing of Alloys and Composites*, eds. H. Möller, G. Govender, South Africa, 2012. Solid State Phenomena 192-193 (2013) 1-574.
7. U.A. Curle *et al.*, *Diff. and Defect Data Pt.B: Solid State Phenom.*, 2013, 192-193: 3.

Table 1: Summary statistics of OLM and SIA particle analyses.

		Population mean	Standard deviation
Roundness	OLM	0.66	0.16
	SIA	0.66	0.12
Aspect ratio	OLM	1.65	0.53
	SIA	1.47	0.27
Ferret length (μm)	OLM	96	72
	SIA	108	50

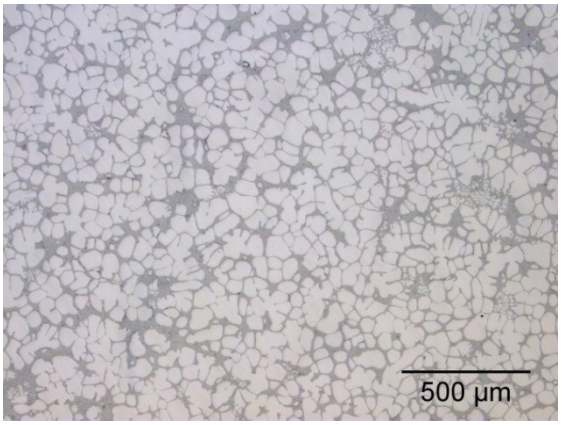

Figure 1: General microstructure of the R-HPDC A356 alloy in the as-cast condition.

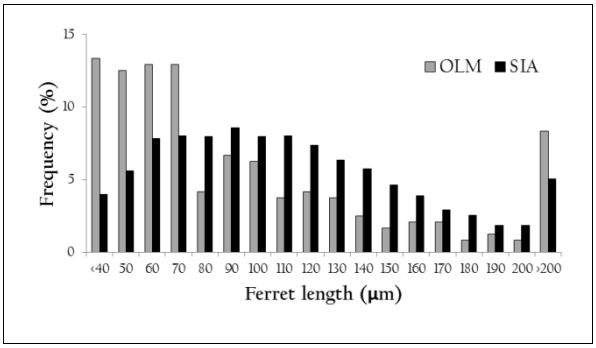

Figure 3: Frequency histogram of ferret lengths of grains observed with OLM and SIA image analyses.

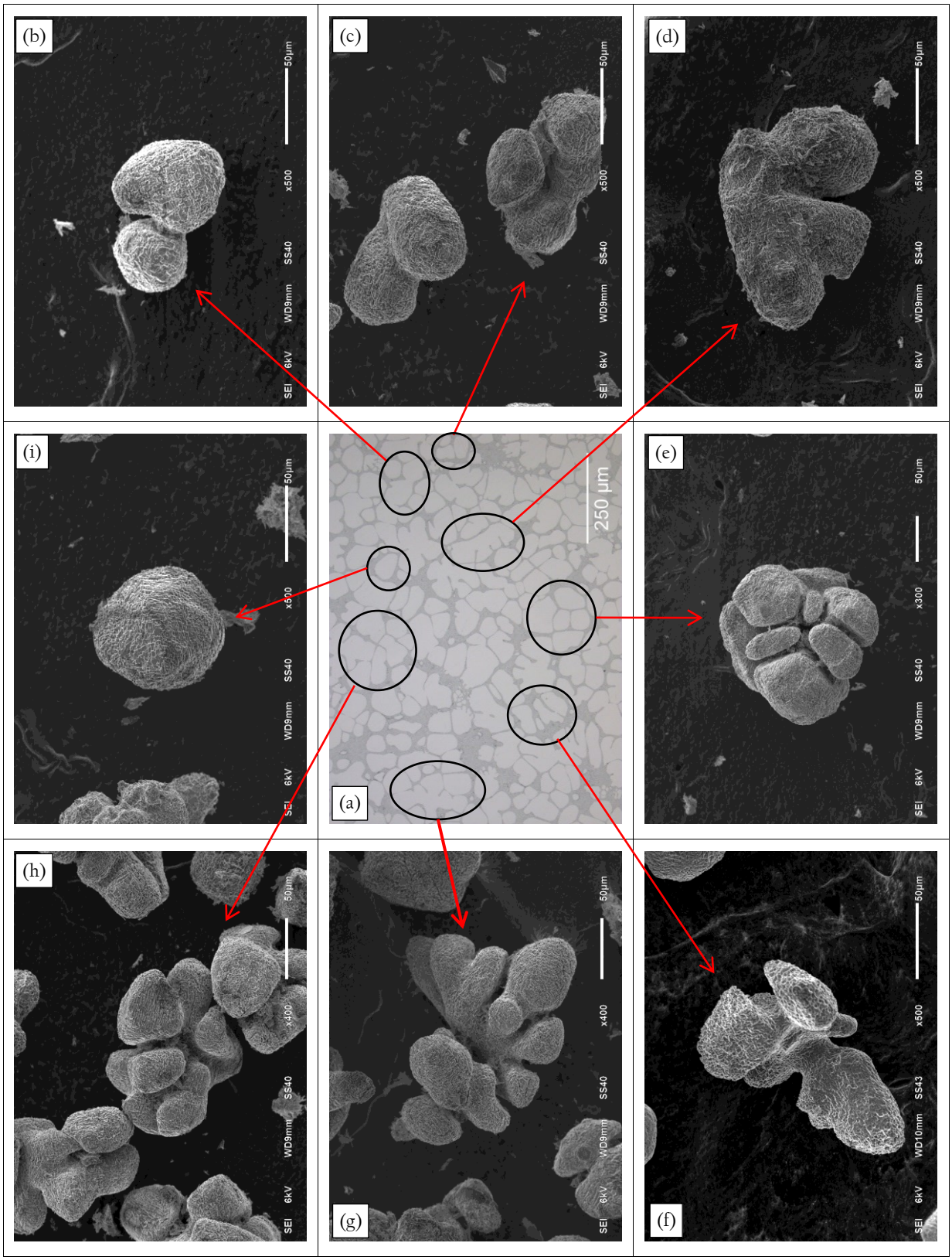

Figure 2: (a) 2D micrograph of the rheo-process and HPDC microstructure, (b)-(i) 3D images of extracted grains from the casting.